Supplementary Information For

Alpha and beta diimine cobalt complexes in isoprene polymerization: a comparative study

Mohammed N. Alnajrani*, Sultan A. Alshmimri and Omar A. Alsager

King Abdulaziz City for Science and Technology (KACST), Kingdom of Saudi Arabia, PO Box 6086, Riyadh 11442.
E-mail: mnajrani@kacst.edu.sa

Content

1. The presence of chain transfer in IP polymerization by A

It was found that the molecular weight increased with polymerization time, but the polydispersity was greater than 2 indicating the presence of chain transfer to monomer. The molecular weight distribution got broader when half of the monomers were converted after one day compared to the beginning of the polymerization where just less than 13% of the monomer was converted. In addition, the molecular weight distribution was monomodal during the first 24 hours, but became bimodal at extended time periods, indicating the presence of chain transfer to polymer (crosslinking); (Fig. 1). Consequently, the molecular weight increased dramatically when the polymerization was carried out for two days (M_w = 7.6 × 10^5 g mol^{-1}).

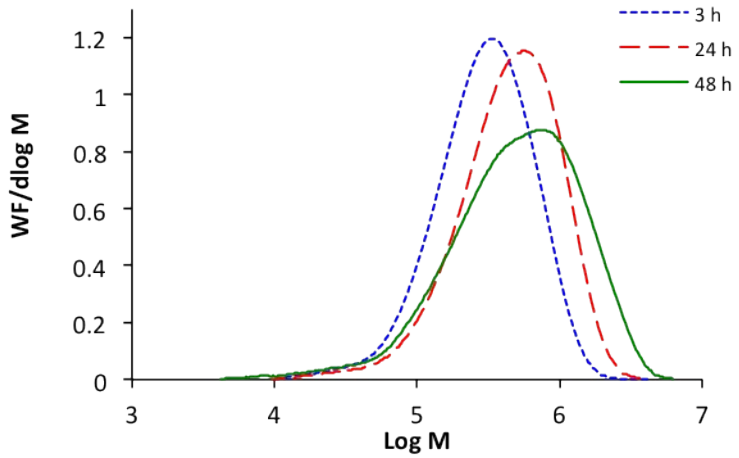

Fig. 1 GPC curves of polyisoprene by **A** at difference times.

As is well-known, several types of chain transfer during the polymerization might happen: either to monomer, aluminum or polymer chain (Chart 1). If it is assumed that at the beginning of the polymerization when the monomer is plentiful, chain transfer to monomer is the only side reaction, then the rate of chain transfer to monomer can be extracted from equation 1, where R_{ctm} = rate of chain transfer to monomer, k_{ctm} = rate constant for chain transfer to monomer and [IP] is the concentration of isoprene.

$$R_{ctm} = k_{ctm}[IP]\,[C^*] \quad \ldots\ldots\ldots (1)$$

To study the presence of chain transfer, the number of chains (N_c) was calculated from equation 2 and then N_c was plotted against polymerization time. The value of N_c increased linearly with polymerization time where just around half of monomers were converted: where monomer was plentiful, chain transfer to monomer dominated. When the polymerization time was extended, N_c levelled off (Fig. 2.a) and the molecular weight distribution of the produced polymer became bimodal. This phenomenon is ascribed to the presence of chain transfer to polymer, where merging between polymer chains led to decrease the value of N_c and then increase the molecular weight. Consequently, the rate of chain transfer to monomer could be derived by taking the gradient of the linear portion (the first four datapoints) of the data; R_{ctm} was found to be 4.54×10^{13} chains s^{-1} (Fig. 2.b).

$$no.\ of\ chains\ at\ time\ t\ (N_C) = \frac{yield\ at\ time\ t\ (g)}{M_n\ (g.mol^{-1})} \times\ Avogadro\ number(mol^{-1}) \quad \ldots\ldots\ldots(2)$$

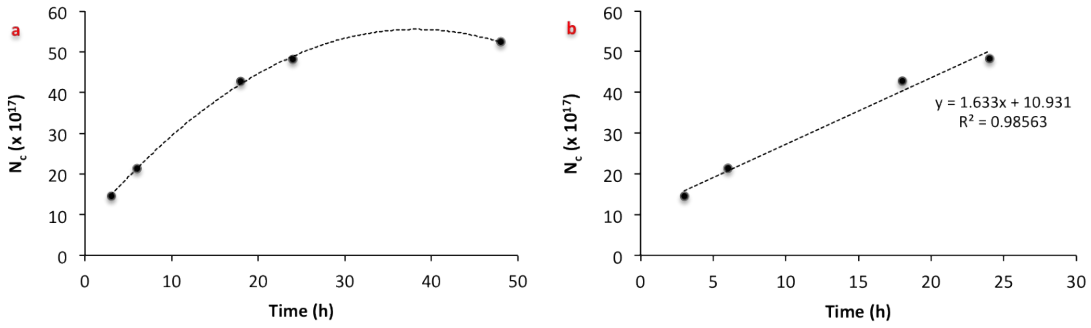

Fig. 2 Plotting of N_c against time for **A**.

The phenomenon described by Boucher *et al*[1] that the value of N_c at zero conversion is equal to the number of active centres (C*) where instantaneous initiation is assumed. This assumption was supported by a rapid colour change observed immediately upon addition of DEAC. The plotting of N_c against conversion (%) is displayed in Fig. 3.a. A linear relationship for the first 24 hours was obtained before N_c leveled off due to chain transfer to polymer after 48 hours. Using just the first four datapoints where chain transfer to monomer was dominant, then the value of C* is equal to the intercept at N_c at zero conversion (Fig. 3.b). Using this method, C* was estimated to be 3.7×10^{17} indicating that approximately 12% of the cobalt complex was activated. This value is essentially identical to that found for β-triimine complexes.[2] Furthermore, the volume of

the polymerization is known (0.035 L) and so [C*] was calculated from equation 3. Therefore, [C*] was found to be 1.76×10^{-5} M. As the values of k and [C*] are known now then we can determine the value of the rate constant of propagation from equation 4; $k_p = 0.43$ s^{-1} M^{-1}.

$$[C^*] = \frac{C^*}{Avogadro\ number(mol^{-1})} \div 0.035\ (L) \quad \text{.....(3)}$$

$$k = k_p \times [C^*] \quad \text{.....(4)}$$

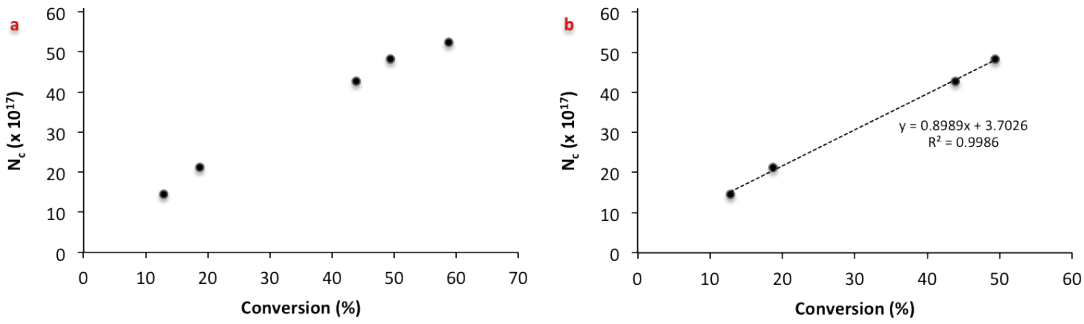

Fig. 3 Plot of N_c against conversion for **A**.

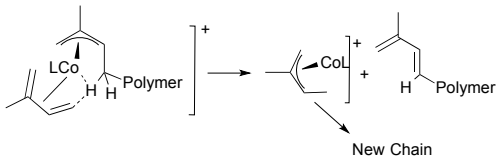

Direct Chain Transfer to Monomer

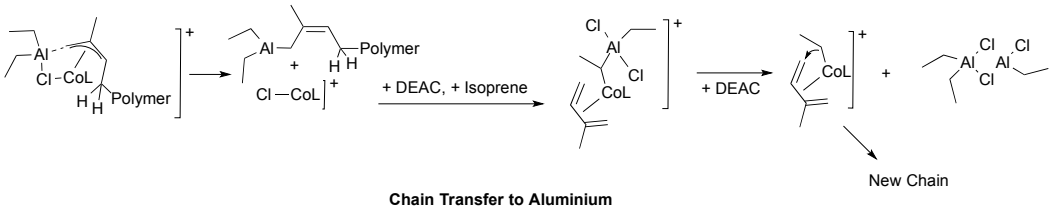

Chain Transfer to Aluminium

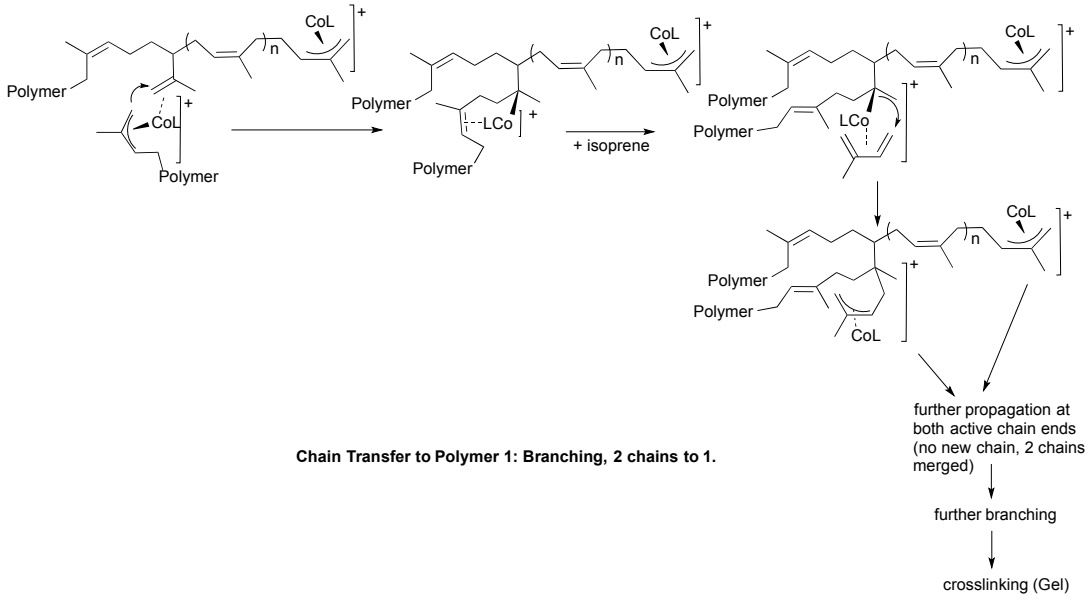

Chain Transfer to Polymer 1: Branching, 2 chains to 1.

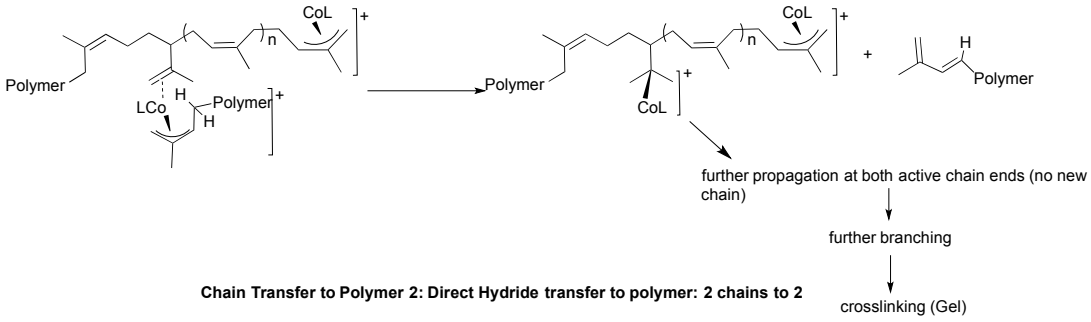

Chain Transfer to Polymer 2: Direct Hydride transfer to polymer: 2 chains to 2

Chart 1 Proposed chain transfer events.

2. The presence of chain transfer in IP polymerization catalysed by B

The value of M_w increased linearly (r^2 = 0.98) with polymerization time while M_n increased only for the first 20 minutes before it leveled off at 1.0×10^5 g mol^{-1}. This behavior was due to chain transfer which can be determined by the value of $Đ$ which was 2.38 when 19% of monomer was converted and became 3.36 when full conversion was obtained. To support this approach, the number of chains (N_c) during the polymerization was calculated for **B** as has already been presented above for **A**. It was found that N_c increased with time for the first 40 minutes where the monomer was plentiful and chain transfer to monomer dominated. As the monomers dwindled the value of N_c leveled off (Fig. 4.a). Consequently, the first four points defined a linear relationship, the gradient of which was equal to the rate of chain transfer to monomer (R_{ctm}), 89.62×10^{14} chains s^{-1} (Fig. 4.b) for **B**.

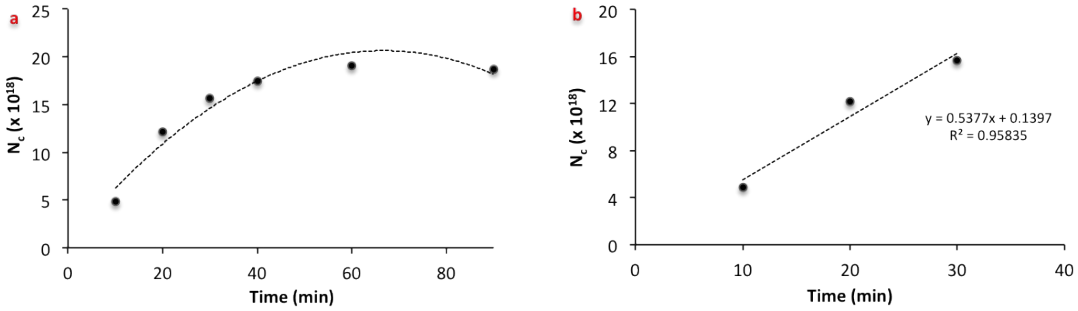

Fig. 4 Plotting of N_c against time for **B**.

Plots of N_c against conversion (%) are displayed in Fig. 5.a. As mentioned above, the N_c increased linearly for the first 40 minutes before it leveled off as the monomer dwindled, indicating a decrease in the rate of chain transfer to monomer. Therefore, the first four datapoints of Fig. 5.a were linear. The value of its intercept at zero conversion was obtained (Fig. 5.b). The value of C* for **B** was found to be 15.457×10^{17}, which means that 51.3% of the cobalt complex present was activated. This value is similar to that found for the bidentate enamine-diimines reported in our previous paper.[3] Although there was no big difference in the percentage of activated sites between **B** and [(2,4,6-$Me_3C_6H_2NH$)MeC=C(CMe_2(2,4,6-$Me_3C_6H_2N)_2CoBr_2$] (**D**) (≈ 50%),[3] there was a remarkable difference in the activity; R_p was 6.75×10^{-5} M s^{-1} for **D** and 1.17×10^{-3} M s^{-1} for **B**. This phenomenon is ascribed to the structure of the ligands, where the greater

ortho bulk of the isopropyl groups in **B** weakens the strength of binding of the allyl chain end, in a manner reminiscent of the activating effect of *ortho* bulk on nickel complexes in ethene polymerization.[4] In the case of [(2,4,6-$Me_3C_6H_2NH$)MeC=C(CMe_2(2,4,6-$Me_3C_6H_2N$)$_2$CoBr(thf)][BArF] (**E**), 47% of cobalt complex was activated meaning also no big difference in the percentage of the active cobalt sites compared to **B**.[3] Therefore, the nature of the counter-ion of the active centre is an essential factor leading **E** (R_p = 1.84 × 10^{-3} M s^{-1}) to be more active than **B**.

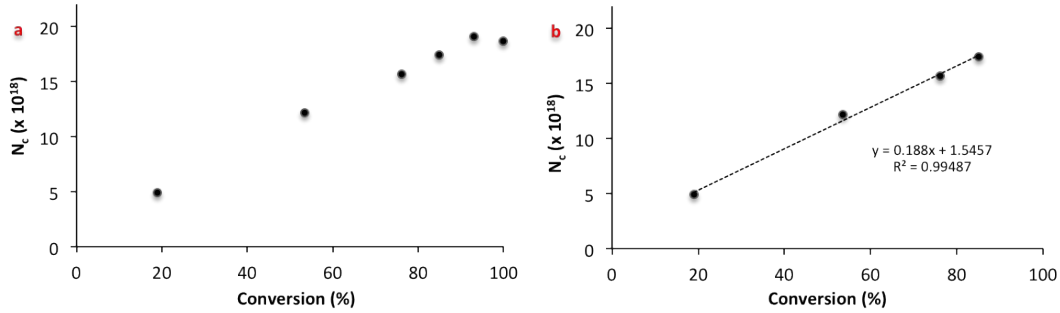

Fig. 5 Plotting of N_c against conversion for **B**.

Moreover, the molecular weight was higher for the polymer produced by **E** compared to **B** with the same yield while *Đ* was lower; as can be seen in Table 1. Therefore, the nature of the active center did not affect just the activity but also the properties of the produced polymer. It is proposed that the counter-ion $[Al]^-$ facilities the chain transfer, whereas $BArF^-$, well-known as a non-coordinating (or weakly coordinating) and large counter-ion, does not have a strong influence on the chain transfer.

Table 1 Comparison between B and E.

Catalyst	Time (min)	Yield (%)	M_w g mol^{-1} ×10^5	M_n g mol^{-1} ×10^5	*Đ*
E	10	52.9	2.9	1.5	1.93
B	20	53.5	2.3	0.9	2.56
E	20	76.0	3.8	1.7	2.24
B	30	76.2	2.5	1.0	2.50
E	35	89.1	4.8	2.0	2.4
B	60	91.0	3.0	1.0	3.0

Interestingly, the molecular weight of polymers produced by **D** and **B** with similar conversion had similar molecular weight (Table 2). This phenomenon might be ascribed

to the nature of counter-ion on the active center. As mentioned before, these two complexes had different ligand structure resulting in different activity, but their counter-ions were similar ($[Al]^-$).

Table 2 Comparison between B and D.

Catalyst	Time	Yield (%)	M_w g mol^{-1} $\times 10^5$	M_n g mol^{-1} $\times 10^5$	$Đ$
D	1 h	19.0	1.9	0.8	2.38
B	10 min	19.0	1.9	0.8	2.38
D	12 h	91.0	3.1	1.0	3.10
B	1 h	91.0	3.0	1.0	3.00

However, the presence of chain transfer to polymer was also observed in IP polymerization by **B**. This side reaction was encouraged as the monomer dwindled. At the beginning of the polymerization, the molecular weight distribution was narrow with only a small tail of low molecular due to chain transfer to monomer. In contrast, at the end of the polymerization where all monomers were consumed, the distribution of the molecular weight was broad and at least bimodal; a high-molecular weight tail was introduced to the distribution because of chain transfer to polymer. This tail grew larger and broader as the polymerization time was extended, just as was seen for **A**, **C** **D** and **E**.[2, 3] For example, a polymerization left for three hours produced a polymer of much higher molecular weight (M_w = 7.0 × 10^5 g mol^{-1} and M_n = 1.7 × 10^5 g mol^{-1}) and broader dispersity ($Đ$ = 4.12) with bimodal molecular weight distribution (Fig. 6) in comparison to more normal polymerization times. The value of M_n after 180 minutes was higher compared to the polymerization for 90 minutes, although in both cases the conversion was 100%. Therefore, equation 2 dictated that the number of chains dropped as the polymerization was carried out for longer time periods (three hours). NMR results of the produced polymers showed the presence of 3,4- enchainment, and it is assumed that this led the active center to coordinate the double bond when the monomer dwindled. As a result, the value of N_c decreased due to chain transfer to polymer and the molecular weight then increased sharply.

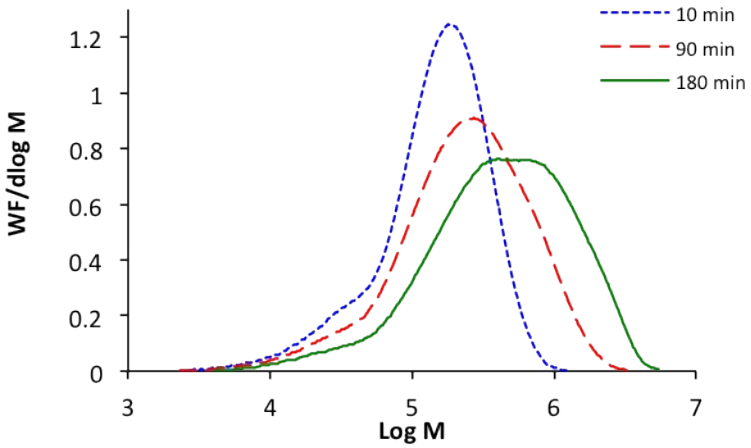

Fig. 6 GPC curves of polyisoprene by **B** at difference times.

Moreover, the value of [C*] was found to be 7.34×10^{-5} M (equation 3). As the values of k and [C*] are known, the value of the rate constant of propagation can be determined from equation 4; $k_p = 11.2$ s^{-1} M^{-1}. The [C*] of **A** was lower compared to **B**, and this was one of the reasons that the molecular weight of the polymer produced by **A** was higher than that of **B** with the same yield (Table 3). Therefore, the initiation step of **A** was inefficient under these conditions. However, the number of active centers was increased by increasing Al mol ratio and also by polymerization temperature (*vide infra* for study of aluminium and temperature effects).

Table 3 Comparison between **A** and **B**.

Catalyst	Time	Yield (%)	M_w g mol^{-1} $\times 10^5$	M_n g mol^{-1} $\times 10^5$	$Đ$
A	6 h	18.7	4.2	1.8	2.33
B	10 min	19.0	1.9	0.8	2.38
A	24 h	49.4	5.8	2.1	2.76
B	20 min	53.5	2.3	0.9	2.56

3. Influences of co-catalyst and [Al]/[Co] mol ratio

3.1. α-Diimine cobalt complex (A)

There was an obvious change in the polymerization solution colour with Al mol ratio. At low loading of Al (≤100) no remarkable change of the solution colour was observed; it remained brownish, which is the colour of solutions of **A**. Increasing Al mol ratio from 150 to 400 resulted in a change in the colour from brownish to greenish and also

the degree of the greenish colour was darkest at 400 mol ratio of Al (Fig. 7). At low Al mol ratio (≤100), the activation stage was inefficient, and only a trace of polymer was produced. Therefore, it was required to add more alkylation reagent to generate more active sites. The activity then increased as the Al ratio increased from 100 to 200 before it decreased at 400 mol ratio (Fig. 8.a). It is assumed that this is a result of aluminium-promoted deactivation. Interestingly, increasing Al mol ratio led to an increase in the molecular weight of the polymer, with a narrow distribution. For instance, when Al/Co was 100, a polymer with $M_n = 9.0 \times 10^4$ g mol^{-1} and $Đ = 2.89$ resulted, while a 200 mol ratio of Al/Co resulted in a polymer of $M_n = 4.3 \times 10^5$ g mol^{-1} and $Đ = 2.00$. The N_c was maximized at 150:1 while further loading of Al resulted in lower N_c (Fig. 8.b).

Fig. 7 The colour of polymerization solution with a different loading of DEAC/**A**.

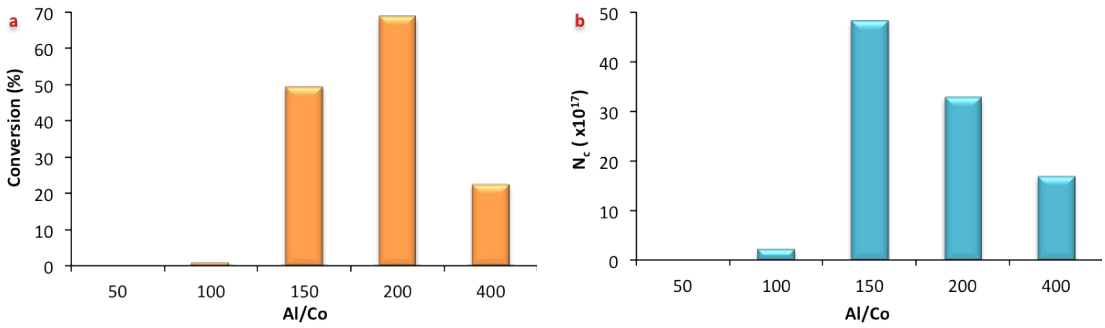

Fig. 8 Plotting of Al/Co mol ratio against: a) conversion and b) N_c, for **A**.

Furthermore, the type of alkylation reagent was also found to have an influence on the activity and the properties of the produced polymer. It was found that EASC/**B** was more active than DEAC/**B**, while the latter produced higher molecular weight ($M_n = 1.8 \times 10^5$ g mol^{-1}) compared to EASC/**B** (5.0×10^3 g mol^{-1}). The molecular weight distributions of the polymers produced by these two systems are displayed in Fig. 9. EASC/**A** resulted in a broad and multimodal molecular weight distribution while the DEAC/**A** system produced a more monomodal distribution. As mentioned in the main paper, the contact ion pairs generated after activation depended on the type of Al anion. Therefore, EASC produced a wider range of active sites resulting in a range of

polymerization rates. Since the only difference between EASC and DEAC is that a dimer has one more chlorine atom, the Cl atoms must play an important role in term of chain transfer (Chart 1), possibly as bridges between Co and Al.

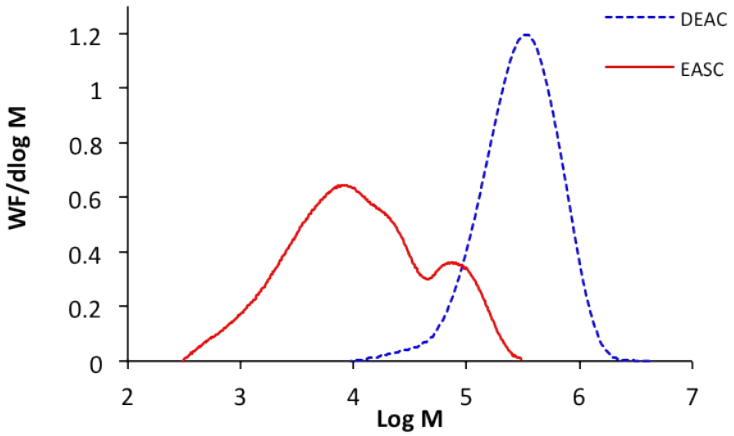

Fig. 9 GPC curves of polyisoprene by DEAC/**A** and EASC/**A** systems.

Moreover, the nature of the alkylation reagent had an influence on the microstructure of the polymer produced by **A**. When DEAC was replaced with EASC, the polymer became predominantly *trans*-1,4 (61.2%), while it was *cis*-1,4 (79.8%) where DEAC was used under identical conditions (Fig. 10).

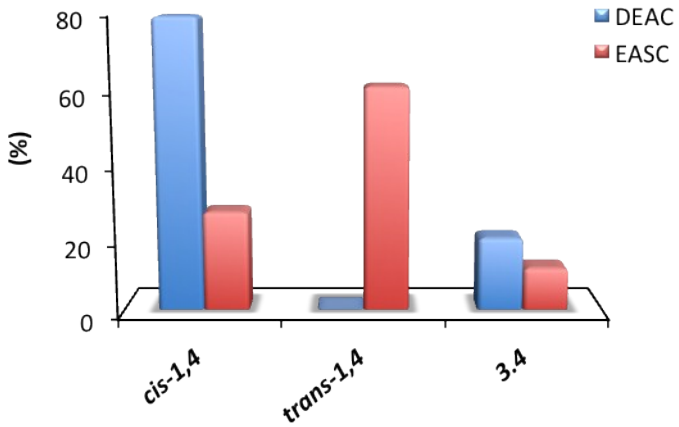

Fig. 10 Microstructure of polyisoprene by DEAC/**A** and EASC/**A** systems.

Since cationic polymerization is known to produce predominantly *trans* polymer, this might be because the higher Lewis Acidity of EASC promoted some cationic polymerization competing with the coordination polymerization on cobalt.

3.2. β-Diimine cobalt complex (B)

In the case of **B**, it was also found that increasing DEAC: Co ratio resulted in low activity (Fig. 11.a). For instance, the conversion was 94.4% when a 25:1 mol ratio was used while it dropped to 32.1% at a 200:1 mol ratio. In addition, the molecular weight was also affected by Al/Co; it decreased as the ratio increased. M_w was 3.4 × 10^5 g mol^{-1} when the ratio was 25:1 and it dropped to 1.9 × 10^5 g mol^{-1} as the ratio increased to 200:1. Consequently, the presence of excess of DEAC appeared to deactivate the active centers leading to a decrease in activity and M_w. Therefore, further addition of Al reagent (DEAC) decreased the number of active sites and lowered M_w. To support this hypothesis, the value of N_c for each polymerization was calculated. N_c was then plotted against Al/Co mol ratio (Fig. 11.b). The number of chain decreased as the mol ratio of Al/Co increased from 25 to 200.

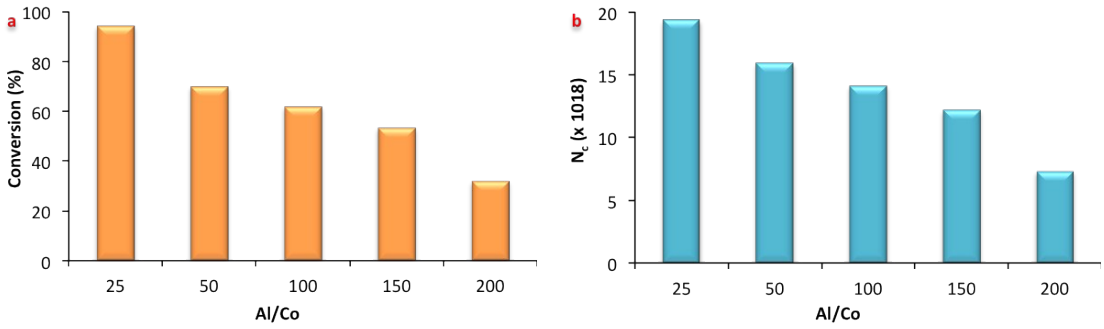

Fig. 11 Plotting of Al/Co mol ratio against: a) conversion and b) N_c, for **B**.

As for **A**, the activity of **B** and the molecular weight were affected by the nature of alkylation reagent, and EASC/**B** was more active than DEAC/**B** while the former produced higher molecular weight (M_n = 9.0 × 10^4 g mol^{-1}) compared to EASC/**B** (M_n = 4.0 × 10^4 g mol^{-1}). The molecular weight distributions of the polymers produced by these two systems are displayed in Fig. 12.

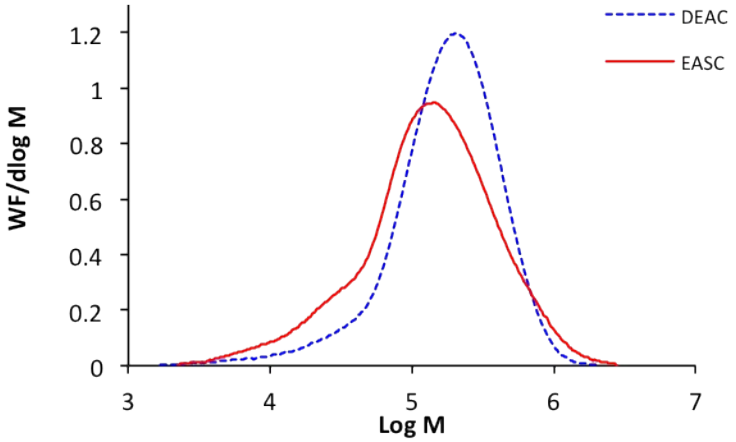

Fig. 12 GPC curves of polyisoprene by DEAC/B and EASC/**B** systems.

4. The effect of polymerization temperature

4.1. α-Diimine cobalt complex (A)

In the case of **A**, both activity and N_c increased with polymerization temperature, and the trend was more of exponential increase then a linear one (Fig. 13). As mentioned in the main paper, increasing the temperature resulted in increase of the number of active centres according to the colour of the polymerization solution and activity value. Moreover, increasing the temperature facilitated the presence of chain transfer to monomer. The values of molecular weight and dispersity showed that M_n decreased linearly (r^2 = 0.97) while $Đ$ increased linearly (r^2 = 0.96) with temperature (Fig. 14). Consequently, polymerization temperature encouraged chain transfer to monomer resulting in a dramatic increase in N_c value as can be seen in Fig. 13.b.

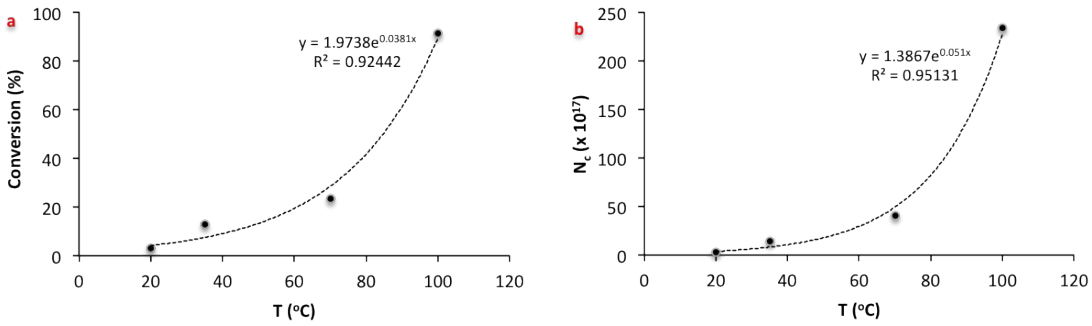

Fig. 13 Plotting of polymerization temperature against: a) conversion and b) N_c, for **A**.

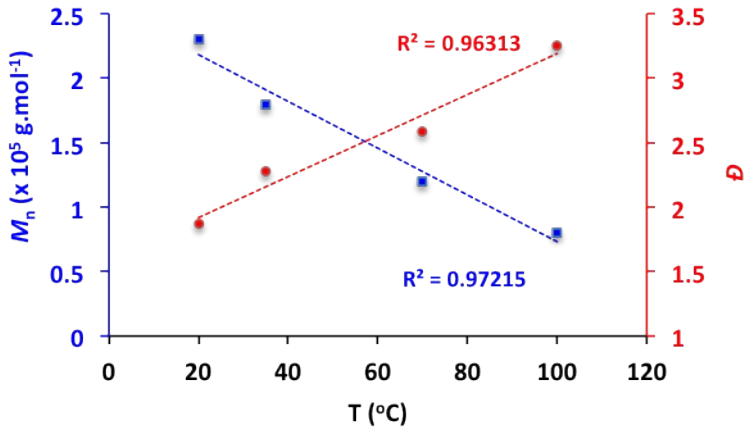

Fig. 14 Plotting M_n and $Đ$ against polymerization temperature, for **A**.

4.2. β-Diimine cobalt complex (B)

The effect of the polymerization temperature was clearly found to have an influence on both activity and molecular weight for **B**. The activity increased linearly from 0 to 35 °C before it leveled off at 70 °C and then decreased at 100 °C. It was noticed that increasing the temperature led to increase N_c. This phenomenon might be ascribed to two reasons or one of them; increase the number of active sites and/or the presence of chain transfer to monomer. Fig. 15.a displays that the polymerization by **B** obeyed Arrhenius behavior in the range of 0 to 35 °C where also the value of N_c increased linearly (Fig. 15.b). Further increase in polymerization temperature did not encourage the activity while N_c sharply increased. With the aid of the values of M_n and $Đ$ at 35 and 70 °C, we can ascribe the increase of N_c at this temperature to chain transfer to monomer. Further increase in the temperature led to reduce both activity and N_c due to de-activation of the active centres (Fig. 15).

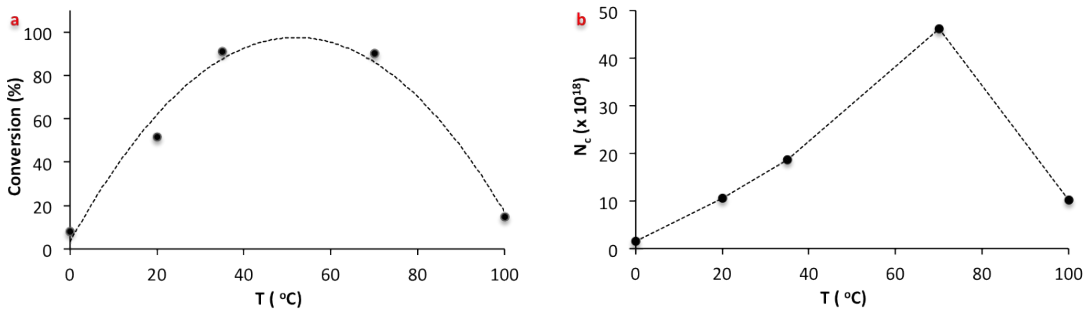

Fig. 15 Plotting of polymerization temperature against: a) conversion and b) N_c, for **B**.

5. Determination of the microstructure of polyisoprene

The obtained polyisoprene was characterized by $^{13}C\{^{1}H\}$NMR in order to investigate its microstructure according with the literature.[5, 6, 7] The spectra of two different samples with different microstructure are displayed in Fig. 16-19. Polyisoprene obtained using DEAC:**A** system at 35 ˚C was approximately 80% *cis*-1,4 enchainment, but there are also significant amounts of 3,4-vinyl and a very small amount of *trans*-1,4-enchained monomers, as shown by Fig. 16 and Fig. 17. The pattern of selectivity and regioerrors after 3,4 linkages are exactly as were reported for **C**, **D** and **E**.[2, 3] Eight distinct monomer triad environments are shown in Chart 2 and the most abundant triads would be A and C. Peaks are labelled according to this key Chart 2.

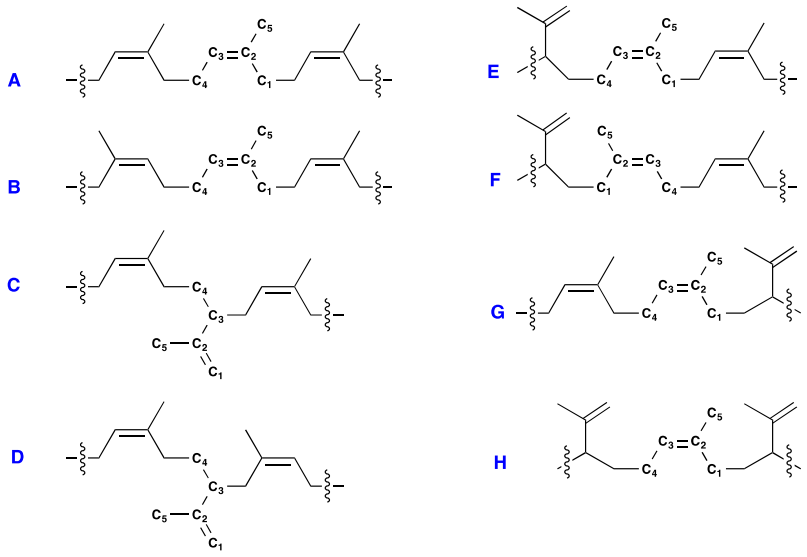

Chart 2 Polymer triads expected in a high *cis*-1,4-polyisoprene.

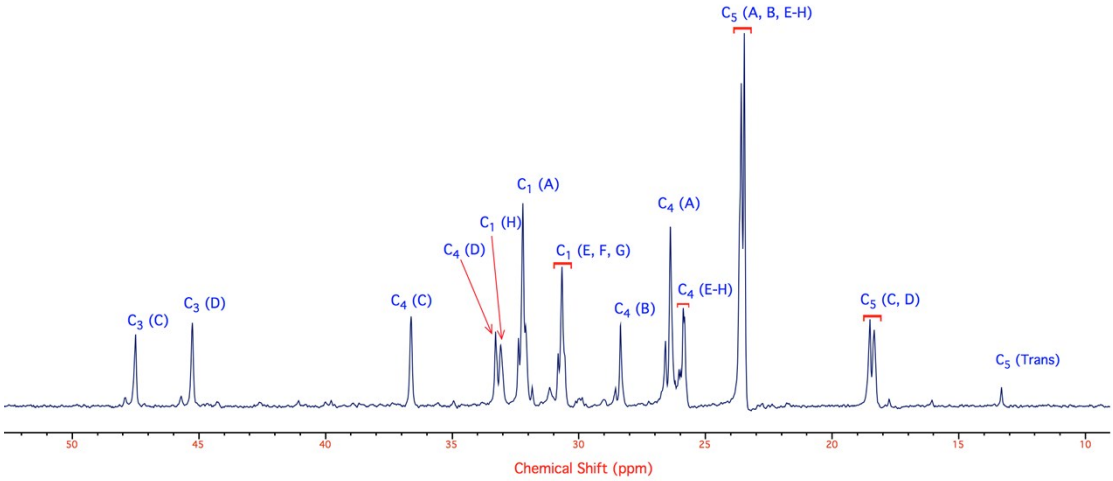

Fig. 16 ^{13}C NMR spectrum (sp^3 region) of PI by DEAC/**A** (*cis*-1.4 = 79.8%; *trans*-1,4 = 0.2%; 3,4 =20.0%).

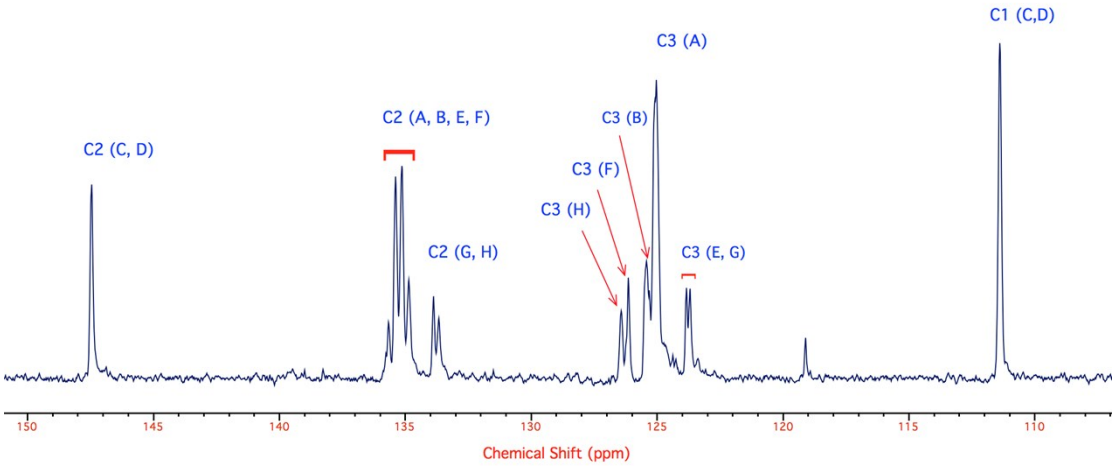

Fig. 17 ^{13}C NMR spectrum (sp^2 region) of PI by DEAC/**A** (*cis*-1.4 = 79.8%; *trans*-1,4 = 0.2%; 3,4 =20.0%).

Polyisoprene obtained using EASC:**A** system at 35 ˚C was approximately 61.2% *trans*-1.4, 27.2% *cis*-1,4 and 11.6% 3,4 (Fig. 18 and Fig. 19). Assignment of the peaks in this high-*trans* polymer requires the definition of further triads incorporating *trans* units. Some of these are shown in Chart 3.

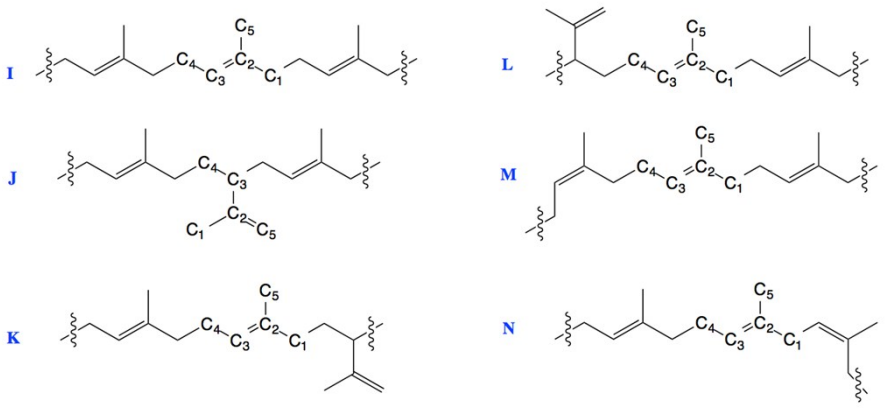

Chart 3 Polymer triads expected in a high *trans*1,4-polyisoprene.

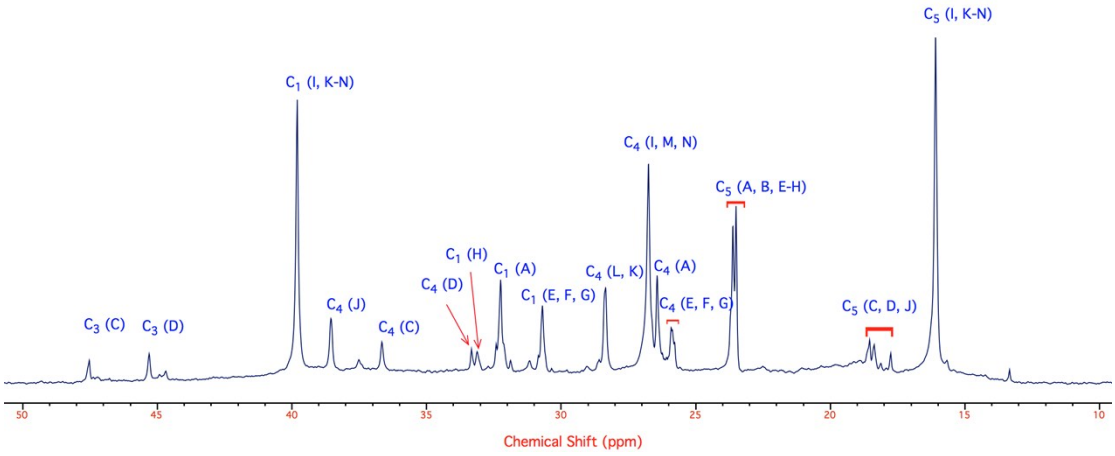

Fig. 18 ^{13}C NMR spectrum (sp^3 region) of PI by EASC/**A** (*cis*-1,4 = 27.2%; *trans*-1,4 = 61.2%; 3,4 =11.6%).

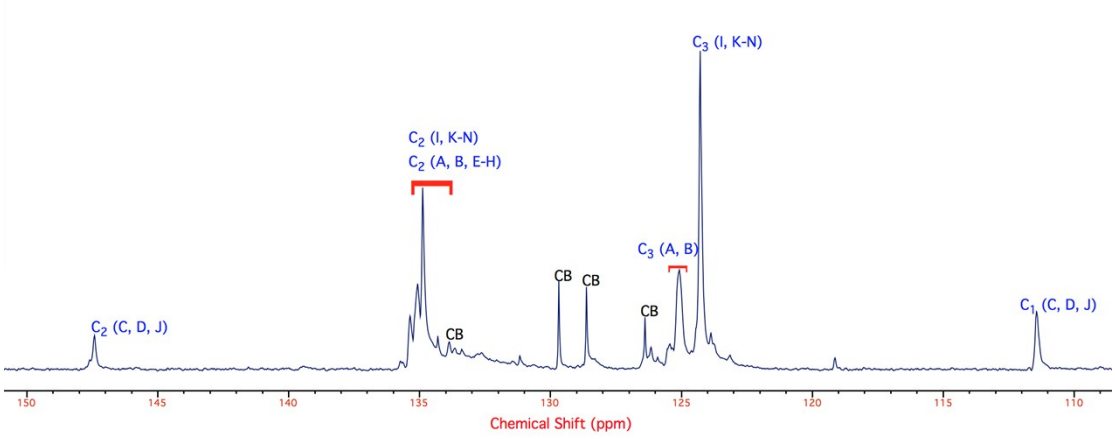

Fig. 19 ^{13}C NMR spectrum (sp^2 region) of PI by EASC/**A** (*cis*-1,4 = 27.2%; *trans*-1,4 = 61.2%; 3,4 =11.6%); CB is chlorobenzene (the polymerization solvent).

6. Crystallographic information

Table 4 Crystallographic information for **A** and **B**.

Identification code	**A**	**B**
Empirical formula	$C_{72}H_{80}Br_4Co_2N_4$	$C_{30}H_{44}Br_2Cl_2CoN_2$
Formula weight	1438.90	722.32
Temperature/K	150	150
Crystal system	monoclinic	monoclinic
Space group	$P2_1/c$	$P2_1/n$
a/Å	27.1936(17)	19.4172(12)
b/Å	12.0960(5)	7.9998(3)
c/Å	22.8296(11)	21.5000(11)
α/°	90	90
β/°	113.511(7)	101.005(5)
γ/°	90	90
Volume/Å^3	6886.0(7)	3278.3(3)
Z	4	4
ρ_{calc}g/cm^3	1.388	1.464
μ/mm^{-1}	2.845	3.145
F(000)	2936.0	1476.0
Crystal size/mm^3	0.1 × 0.1 × 0.05	0.1 × 0.1 × 0.05
Radiation	MoKα (λ = 0.71073)	MoKα (λ = 0.71073)
2Θ range for data collection/°	5.852 to 52.744	6.284 to 52.744
Index ranges	$-30 \le h \le 33$, $-15 \le k \le 12$, $-28 \le l \le 28$	$-20 \le h \le 24$, $-7 \le k \le 9$, $-20 \le l \le 26$
Reflections collected	32705	15496
Independent reflections	14054 [R_{int} = 0.0417, R_{sigma} = 0.0631]	6695 [R_{int} = 0.0346, R_{sigma} = 0.0551]
Data/restraints/parameters	14054/0/755	6695/0/344
Goodness-of-fit on F^2	1.143	1.022
Final R indexes [I>=2σ (I)]	R_1 = 0.0751, wR_2 = 0.1654	R_1 = 0.0450, wR_2 = 0.0803
Final R indexes [all data]	R_1 = 0.1040, wR_2 = 0.1763	R_1 = 0.0759, wR_2 = 0.0904
Largest diff. peak/hole / e Å^{-3}	1.06/-0.65	0.94/-0.74

7. References

1. F. Ghiotto, C. Pateraki, J. R. Severn, N. Friederichs and M. Bochmann, *Dalton Trans.*, 2013, **42**, 9040.
2. M. N. Alnajrani and F. S. Mair, *RSC Advances*, 2015, **5**, 46372.
3. M. N. Alnajrani and F. S. Mair., *Dalton Trans*., 2016, **45**, 10435.
4. J. Feldman, S. J. McLain, A. Parthasarathy, W. J. Marshall, J. C. Calabrese and S. D. Arthur, *Organometallics*, 1997, **16**, 1514.
5. Y. Hu, W. Dong and T. Masuda, *Macromol. Chem. Phys.*, 2013, **214**, 2172.
6. Y. Hu, C. Zhang, X. Liu, K. Gao, Y. Cao, C. Zhang and X. Zhang, *J. Appl. Polym. Sci.*, 2014, **131**, 40153.
7. V. A. Rozentsvet, A. S. Khachaturov and V. P. Ivanova, *Polym. Sci. Ser. A*, 2009, **51**, 870.